flocculonodular lobes were consistent with the development of an unsteady gait and absence of nystagmus, respectively, in both subjects.

Marked immunostaining of MRE11 and NBS1 has been reported in the nucleus of Purkinje cells and Bergmann glial cells in the human brain [10]. Nuclear expression of MRE11 and NBS1 has also been detected in pyramidal neurons of the cerebral cortex in aged adults without dementia and was severely reduced in the cerebral cortex in cases of Alzheimer's disease [14]. In the present study, neurons in multiple brain regions, other than the Purkinje cells and cortical pyramidal neurons showed nuclear immunoreactivity for MRE11 in control brains. As expected, both subjects with ATLD had complete loss of such MRE11 immunoreactivity in the cerebral and cerebellar cortex. Constitutive localization of ATM in human Purkinje cells has been discussed previously [3, 16], and widespread expression of ATM mRNA in the adult human brain has also been reported [18]. In addition, various brain regions, such as the cerebral cortex, thalamus, cerebellum, and pons demonstrated ATM protein expression in Western blot analyses [10]. There seems to be a missing link between the global expressions of MRE11 and ATM in the brain and the selective vulnerability of cerebellar cortex in ATLD and AT. Experiments with *Atm*-null mice showed abnormal differentiation of the Purkinje cells and deficient motor learning, indicating cerebellar dysfunction; however, gross cerebellar degeneration was not seen [5]. The in vitro survival of cerebellar Purkinje cells in both the *Atm* knockout and *Atm* knockin mice was significantly reduced, and most of the Purkinje neurons from the *Atm*-deficient mice showed reduced dendritic branching [6]. These findings suggest the interrelationship between ATM deficiency and Purkinje cell damage in AT. On the other hand, knocking out *Mre11* and the murine ortholog of *NBS1* (*Nbn*) leads to embryonic lethality [28, 29], and *Mre11*- and *Nbn* hypomorphic mutant mice that survive, do not reproduce the neuronal disorders [23, 26]. Recently, it has been reported that conditional inactivation of the *Nbn* in the brain causes microcephaly and cerebellar ataxia [8]. Similar conditional disruption of *Mre11* in murine brains will provide a clue for understanding the interrelationship between MRE11 deficiency and selective cerebellar degeneration.

Reactive-oxygen species are one of the principal damaging agents of neuronal genomic and mitochondrial DNA in the brain, and disturbance of DNA repair activity in neurons, including ATM and MRN complex, can lead to oxidative DNA damage [2, 4]. Oxidative stress has been consistently associated with various neurodegenerative disorders [12]. In xeroderma pigmentosum and Cockayne's syndrome caused by an inherited disturbance in the nucleotide excision repair mechanism, abnormal accumulation of oxidative products was found in the globus pallidus and cerebellar dentate nucleus [11]. Similarly, *Atm*-deficient cells are hypersensitive to oxidative-stress-inducing agents [21]. The cerebellum in *Atm*-deficient mice showed progressive accumulation of DNA strand breaks and decrease in the reduced and oxidized forms of NAD in the brains, leading to perturbation in the balance of pyridine nucleotides [19]. Antioxidants prevented Purkinje cell death in the aforementioned *Atm*-deficient mice and enhanced the levels of dendritogenesis to that in wild-type mice [6]. These data indicate that ATM deficiency can enhance oxidative stress and cause oxidative stress-related neuronal death. Both subjects in our study had increased expression of the DNA marker of oxidative stress, 8-OHdG, in the nuclei of granule cells and Bergmann glial cells, which are structurally and functionally associated with Purkinje cells. Notably, 8-OHdG expression was absent in the severely affected cerebellar cortex, and other brain regions did not show accumulation of oxidative stress markers, except for 4-HNE and AGE in areas with pseudocalcification in subject 1. Therefore, increased oxidative DNA injury is likely to be involved in the selective degeneration of Purkinje cells. Finally, we speculate that the combination of MRE11 deficiency and oxidative DNA injury may lead to selective cerebellar damage in both subjects.

References

1. Ball LG, Xiao W (2005) Molecular basis of ataxia telangiectasia and related diseases. Acta Pharmacol Sin 26:897–907
2. Barzilai A, Biton S, Shiloh Y (2008) The role of the DNA damage response in neuronal development, organization maintenance. DNA Repair 7:1010–1027
3. Biton S, Dar I, Mittelman L, Pereg Y, Barzilai A, Shiloh Y (2006) Nuclear ataxia-telangiectasia mutated (ATM) mediates the cellular responses to DNA double strand breaks in human neuron-like cells. J Biol Chem 281:17482–17491
4. Biton S, Barzilai A, Shiloh Y (2008) The neurological phenotype of ataxia-telangiectasia: solving a persistent puzzle. DNA Repair 7:1028–1038
5. Borghesani PR, Alt FW, Bottaro A, Davidson L, Aksoy S, Rathbun GA, Roberts TM, Swat W, Segal RA, Gu Y (2000) Abnormal development of Purkinje cells and lymphocytes in *Atm* mutant mice. Proc Natl Acad Sci USA 97:3336–3341
6. Chen P, Peng C, Luff J, Spring K, Watters D, Bottle S, Furuya S, Lavin MF (2003) Oxidative stress is responsible for deficient survival and dendritogenesis in Purkinje neurons from ataxia-telangiectasia mutated mice. J Neurosci 23:11453–11460
7. Crawford TO (1998) Ataxia telangiectasia. Semin Pediatr Neurol 5:287–294
8. Frappart PO, Tong WM, Demuth I, Radovanovic I, Herceg Z, Aguzzi A, Digweed M, Wang ZQ (2005) An essential function for NBS1 in the prevention of ataxia and cerebellar defects. Nat Med 11:538–544
9. Frappart PO, McKinnon PJ (2006) Ataxia-telangiectasia and related disorders. Neuromolecular Med 8:495–511

10. Gorodetsky E, Calkins S, Ahn J, Brooks PJ (2007) ATM, the MRE11/Rad50/Nbs1 complex, and topoisomerase I are concentrated in the nucleus of Purkinje neurons in the juvenile human brain. DNA Repair 6:1698–1707
11. Hayashi M (2008) Role of oxidative stress in xeroderma pigmentosum. In: Ahmad SI, Hanaoka F (eds) Molecular mechanisms of xeroderma pigmentosum. Landes Bioscience, Austin, pp 120–127
12. Hayashi M (2009) Oxidative stress in developmental brain disorders. Neuropathology 29:1–8
13. Iijima K, Ohara M, Seki R, Tauchi H (2008) Dancing on damaged chromatin: functions of ATM and the RAD50/MRE11/NBS1 complex in cellular responses to DNA damage. J Radiat Res 49:451–464
14. Jacobson E, Beach T, Shen Y, Li R, Chang Y (2004) Deficiency of the Mre11 DNA repair complex in Alzheimer's disease brain. Brain Res Mol 28:1–7
15. Lammens M, Hiel JA, Gabreels FJ, van Engelen BG, van den Heuvel LP, Weemaes CM (2003) Nijmegen breakage syndrome: a neuropathological study. Neuropediatrics 34:189–193
16. Oka A, Takashima S (1998) Expression of the ataxia-telangiectasia gene (ATM) product in human cerebellar neurons during development. Neurosci Lett 252:195–198
17. Shull ER, Lee Y, Nakane H, Stracker TH, Zhao J, Russel HR, Petrini JH, Mckinnon PJ (2009) Differential DNA damage signaling accounts for distinct neural apoptotic responses in ATLD and NBS. Genes Dev 23:171–180
18. Soares HD, Morgan JI, McKinnon PJ (1998) *Atm* expression patterns suggest a contribution from the peripheral nervous system to the phenotype of ataxia-telangiectasia. Neuroscience 86:1045–1054
19. Stern N, Hochman A, Zemach N, Weizman N, Hammel I, Shiloh Y, Rotman G, Barzilai A (2002) Accumulation of DNA damage and reduced levels of nicotine adenine dinucleotide in the brains of *Atm*-deficient mice. J Biol Chem 277:602–608
20. Stewart GS, Maser RS, Stankovic T, Bressan DA, Kaplan MI, Jaspers NG, Raams A, Byrd PJ, Petrini JH, Taylor AM (1999) The DNA double-strand break repair gene *hMRE11* is mutated in individuals with an ataxia-telangiectasia-like disorder. Cell 99:577–587
21. Takao N, Li Y, Yamamoto K (2000) Protective roles for ATM in cellular response to oxidative stress. FEBS Lett 472:133–136
22. Taylor AM, Groom A, Byrd PJ (2004) Ataxia-telangiectasia-like disorder (ATLD)–its clinical presentation and molecular basis. DNA Repair 3:1219–1225
23. Theunissen JW, Kaplan MI, Hunt PA, Williams BR, Ferguson DO, Alt FW, Petrini JH (2003) Checkpoint failure and chromosomal instability without lymphomagenesis in $Mre11^{ATLD1/ATLD1}$ mice. Mol Cell 12:1511–1523
24. Uchisaka N, Takahashi N, Sato M, Kikuchi A, Mochizuki S, Imai K, Nonoyama S, Ohara O, Watanabe F, Mizutani S, Hanada R, Morio T (2009) Two brothers with ataxia-telangiectasia-like disorder with lung adenocarcinoma. J Pediatr 155:435–438
25. Van de Kaa CA, Weemaes CM, Wesseling P, Schaafsma HE, Haraldsson A, De Weger RA (1994) Postmortem findings in the Nijmegen breakage syndrome. Pediatr Pathol 14:787–796
26. Williams BR, Mirzoeva OK, Morgan WF, Lin J, Dunnick W, Petrini JH (2002) A murine model of Nijmegen breakage syndrome. Curr Biol 12:648–653
27. Williams RS, Moncalian G, Williams JS, Yamada Y, Limbo O, Shin DS, Groocock LM, Cahill D, Hitomi C, Guenther G, Moiani D, Carney JP, Russell P, Tainer JA (2008) Mre11 dimers coordinate DNA end bridging and nuclease processing in double-strand-break repair. Cell 135:97–109
28. Xiao Y, Weaver DT (1997) Conditioned gene targeted deletion by Cre recombinase demonstrates the requirement for the double-stranded break repair Mre11 protein in murine embryonic stem cells. Nucleic Acids Res 25:2985–2991
29. Zhu J, Petersen S, Tessarollo L, Nussenzweig A (2001) Targeted disruption of the Nijmegen breakage syndrome gene *NBS1* leads to early embryonic lethality in mice. Curr Biol 11:105–109

DNA Lesions Induced by Replication Stress Trigger Mitotic Aberration and Tetraploidy Development

Yosuke Ichijima[1], Ken-ichi Yoshioka[1,2]*, Yoshiko Yoshioka[1], Keitaro Shinohe[1], Hiroaki Fujimori[1,2], Junya Unno[3], Masatoshi Takagi[3], Hidemasa Goto[4], Masaki Inagaki[4], Shuki Mizutani[3], Hirobumi Teraoka[1]

1 Department of Pathological Biochemistry, Medical Research Institute, Tokyo Medical and Dental University, Tokyo, Japan, **2** Biochemistry Division, National Cancer Center Research Institute, Tokyo, Japan, **3** Department of Pediatrics and Developmental Biology, Tokyo Medical and Dental University Graduate School, Tokyo, Japan, **4** Division of Biochemistry, Aichi Cancer Center Research Institute, Nagoya, Japan

Abstract

During tumorigenesis, cells acquire immortality in association with the development of genomic instability. However, it is still elusive how genomic instability spontaneously generates during the process of tumorigenesis. Here, we show that precancerous DNA lesions induced by oncogene acceleration, which induce situations identical to the initial stages of cancer development, trigger tetraploidy/aneuploidy generation in association with mitotic aberration. Although oncogene acceleration primarily induces DNA replication stress and the resulting lesions in the S phase, these lesions are carried over into the M phase and cause cytokinesis failure and genomic instability. Unlike directly induced DNA double-strand breaks, DNA replication stress-associated lesions are cryptogenic and pass through cell-cycle checkpoints due to limited and ineffective activation of checkpoint factors. Furthermore, since damaged M-phase cells still progress in mitotic steps, these cells result in chromosomal mis-segregation, cytokinesis failure and the resulting tetraploidy generation. Thus, our results reveal a process of genomic instability generation triggered by precancerous DNA replication stress.

Citation: Ichijima Y, Yoshioka K-i, Yoshioka Y, Shinohe K, Fujimori H, et al. (2010) DNA Lesions Induced by Replication Stress Trigger Mitotic Aberration and Tetraploidy Development. PLoS ONE 5(1): e8821. doi:10.1371/journal.pone.0008821

Editor: Mikhail V. Blagosklonny, Roswell Park Cancer Institute, United States of America

Received October 8, 2009; **Accepted** December 18, 2009; **Published** January 21, 2010

Funding: This study was supported by the Ministry of Education, Culture, Sports, Science and Technology (MEXT) KAKENHI (20770136, 20659047). The funders had no role in study design, data collection and analysis, decision to publish, or preparation of the manuscript.

Competing Interests: The authors have declared that no competing interests exist.

* E-mail: kyoshiok@ncc.go.jp

Introduction

Genomic instability is observed in most cancer cells [1]. In the earliest stages of cancer development, cells exhibit DNA lesions, which are characterized as precancerous DNA lesions and are induced by DNA replication stress with the accelerated cell cycle progression as the results of oncogene acceleration or of aberrant growth activation [2,3]. During these stages, although anti-cancer barrier reactions including cell cycle arrest and inductions of senescence and apoptosis are also competitively activated to block the tumorigenesis step progression [2,3], genomic instability is subsequently started to appear prior to the development of cancer [2,3]. However, the process by which precancerous lesions cause genomic instability remains unclear.

The most common types of genomic instability in cancer cells are alterations in the number of chromosomes, i.e., aneuploidy [4]. Aneuploidy is suggested to develop via unstable intermediates of tetraploidy [5,6]. In addition, tetraploidy even contributes to tumourigenecity *in vivo* [7]. Therefore, the process to generate tetraploidy must be a critical step for the development of many cancers. Furthermore, consistent with the hypothesis of aneuploidy development via unstable tetraploidy intermediates, cancer cells with chromosomal instability show the characteristics of continuous alteration in chromosomal status, highlighting the question for the initiation and the induction of tetraploidy.

Although it is elusive how tetraploidy is developed during cellular transformation, tetraploidy is often observed in cells lacking in the M-phase function [8], which also promotes tumourigenesis [9,10]. Spontaneous tetraploidization is also observed in association with chromosome bridges during mitotic chromosome segregation and the resulting cytokinesis failure [11]. Since the appearance of precancerous lesions is followed by the development of genomic instability [2,3], we hypothesized here that, prior to cellular transformation, precancerous DNA lesions are carried over into the M phase, causing mitotic aberrations, including chromosome-bridge formation to lead into tetraploidy generation, contributing cancer development (Supplementary Fig. S1).

For the above hypothesis, we investigated effects of DNA replication stress-associated lesions by oncogene acceleration or by hydroxyurea treatment as well as impacts of DNA lesions in the M phase, and also studied the immortalization process of primary mouse embryonic fibroblasts (MEFs). Here, we found that DNA replication stress-associated lesions can be transmitted into the M phase, unlike directly induced DNA double-strand breaks, resulting in successive chromosomal mis-segregation, cytokinesis failure and tetraploidy generation. Importantly, we observed that these happen during cellular immortalization, and found that senescing cells are temporarily accumulated with bi-nuclear tetraploidy, which is a form right after the tetraploidy generation, prior to the acquirement of the immortality.

Results

DNA Lesions Induced by Oncogenes Accumulate in the M Phase

To test the above hypothesis (Supplementary Fig. S1), we initiated a study of DNA lesions induced by oncogenes, such as *E2F1*, because the initial stages of cancer development are mimicked by oncogene-acceleration, in which genomic instability is subsequently developed [2]. To determine the effects of the accelerated oncogene function, the spontaneous accumulation of M-phase DNA lesions was monitored with a double staining of γH2AX, a DNA-damage marker, and histone H3 phosphorylated at Ser 10 (p-H3), an M-phase marker (Fig. 1). *E2F1* acceleration caused DNA lesions in U2OS cells (Fig. 1A, B), mimicking the initial stages of cancer development as previously reported [2]. In addition, we observed that these induced DNA lesions are accumulated in mitotic cells (Fig. 1A, C). Similar results were also observed by using another oncogene *Cdc25A* in HEK293 cells (Fig. 1D, E; Supplementary Fig. S2). Thus, supporting our hypothesis (Supplementary Fig. S1), these results show that oncogenic DNA lesions are also appeared in the M phase and indicate the close correlation between mitotic precancerous DNA lesions and genomic instability development.

Oncogene Acceleration Induces Chromosome-Bridge and Aneuploidy

To explore the possible correlation between mitotic DNA lesions and the induction of genomic instability, we determined the appearance of chromosome bridges, because a recent study has shown that spontaneous tetraploidization is triggered by chromosome bridges [11], though it remains elusive how chromosome bridges are induced. After *E2F1* acceleration, we observed chromosome bridges (Fig. 2A) concomitantly with the elevation of polyploidy fraction (Fig. 2B). Intriguingly, such a chromosome bridge was observed with γH2AX signal on the chromosome (Fig. 2A), indicating the involvement of DNA lesions in the

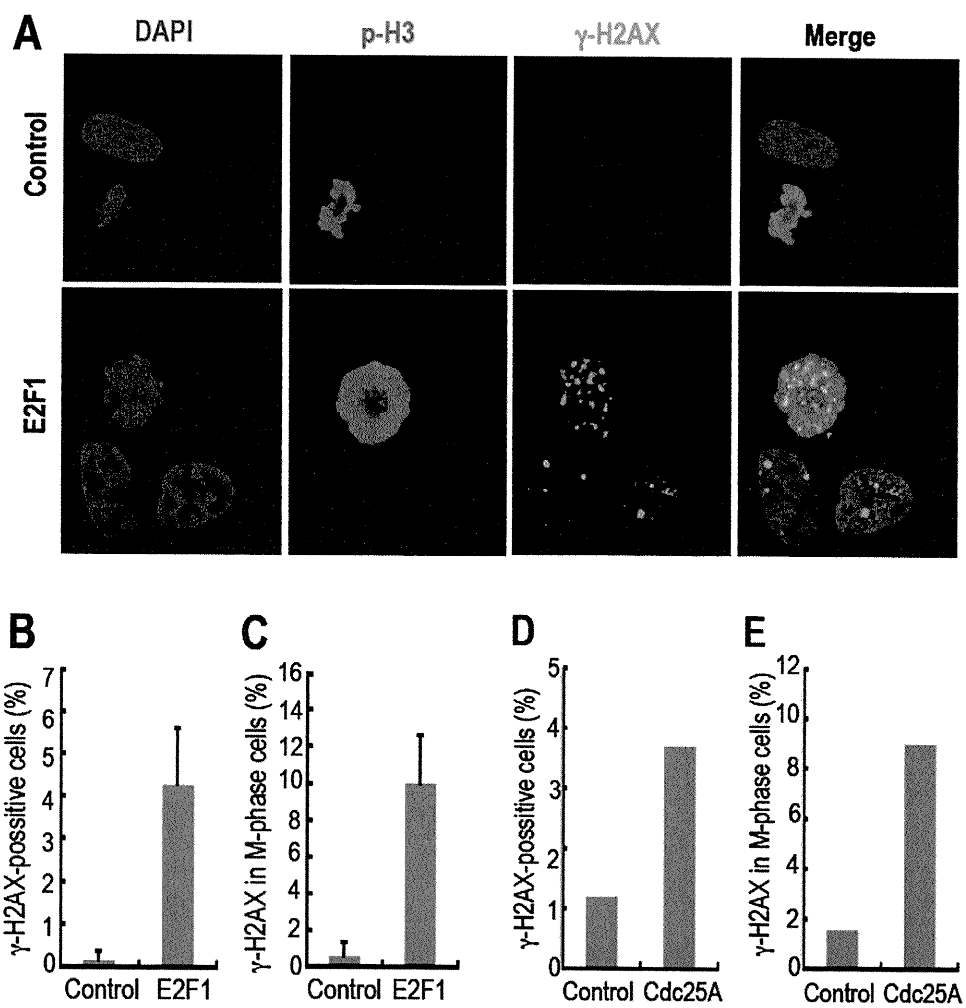

Figure 1. DNA lesions induced by oncogene acceleration are accumulated in the M phase. A. DNA lesions in the M phase were determined by a double staining of γH2AX and p-H3 after nocodazole treatment (100 ng/ml, 12 h). Using ER-*E2F1*-expressing U2OS cells, DNA lesion-carryover into the M phase was evaluated after treatment with 4-hydroxytamoxifen for 6 h (E2F1). Representative images are shown before (control) and after E2F1 activation (E2F1). **B,C.** The proportions of total γH2AX-positive cells (**B**) and γH2AX/p-H3 double-positive cells (**C**) were estimated in the cells prepared as in **A**. At least 50 cells were counted in each of 3 independent experiments. Error bars represent ± SD. **D,E.** Transient over-expression of *Cdc25A* promotes DNA lesions including the cells during mitosis. The proportions of total γH2AX-positive cells (**D**) and γH2AX/p-H3 double-positive cells (**E**) were estimated by counting at least 60 cells in **D** and 500 cells in **E**. Representative fluorescent microscope images are also shown in supplementary Fig. S2.
doi:10.1371/journal.pone.0008821.g001

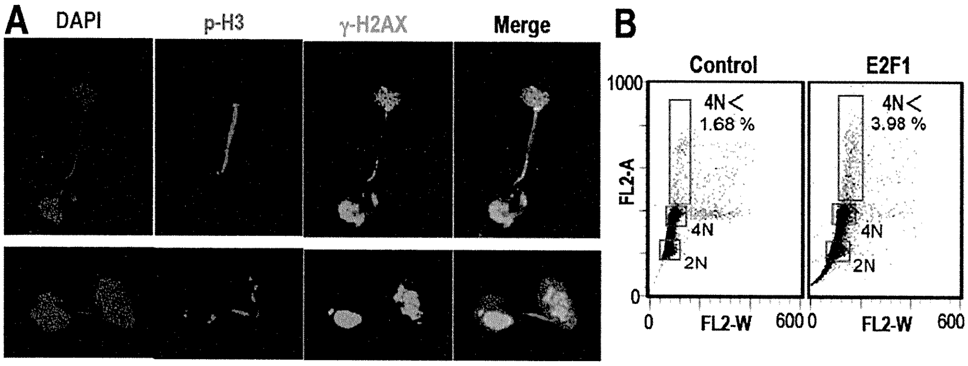

Figure 2. E2F1 acceleration generates chromosome bridge and aneuploidy. A. After E2F1 activation as in Figure 1A, chromosome bridges were often observed with the generated DNA lesions by E2F1 activation. Representative images are shown. B. Cells containing more than 4N DNA content were detected by flow cytometry in the cells treated as in Figure 1A. The proportions of cells with DNA content of 2N, 4N and more (4N<) are indicated by red squares. The percentages of 4N< cells are indicated. The sub-G1 fraction was also observed in E2F1-activated cells.
doi:10.1371/journal.pone.0008821.g002

chromosome bridge formation. Taken together, these results support our hypothesis (Supplementary Fig. S1) and indicate that precancerous DNA lesions induced by oncogenes trigger chromosome bridges during mitosis and induce genomic instability. However, oncogene activation primarily accelerates S-phase entry, thereby the resulting DNA lesions are primarily associated with DNA replication stress in the S phase [2]. Here, an important question arose, if the observed M-phase lesions possibly transmit into the M phase from the S phase with the bypass of cell cycle checkpoints.

DNA Replication Stress-Associated Lesions Transmit into the M Phase

To directly determine the potential of DNA lesion-carryover generated by DNA replication stress in the S phase, we transiently treated the normal human fibroblast SuSa with hydroxyurea (HU) to cause replication fork stalling and the resulting DNA double-strand breaks. After the transient replication stress, γH2AX foci were evidently increased in the subsequent M phase (Fig. 3A,B), showing that DNA lesions induced by replication stress actually transmit into the M phase. However, an important question remains: How can DNA lesions generated by replication stress be carried over into the M phase, despite the existence of the firmly established intra-S and G2/M checkpoints?

Recently, DNA lesion-carryover into the M phase has been shown with fewer than 20 foci of γH2AX per nucleus in the ATM-mutated background after X-ray or γ-ray irradiation [12], implying that cell cycle checkpoints are bypassed under a small number of lesions with compromised damage checkpoint response. To determine the status of DNA lesions and checkpoint activation, we compared γH2AX signals and phosphorylated ATM (p-ATM) signals after *E2F1* acceleration with those of the radiomimetic agent neocarzinostatin (NCS) that causes G2-arrest. While NCS causes γH2AX and the resulting p-ATM foci in the entire nucleus, *E2F1* acceleration was found to cause only very limited γH2AX (Fig. 4A) and the resulting much weaker and limited p-ATM foci (Fig. 4B), indicating only local checkpoint activation. Taken together, our results suggest that DNA lesions induced by replication stress under *E2F1* acceleration, unlike directly induced DNA double-strand breaks, impact a small number of DNA lesions, resulting in limited damage checkpoint response, bypass of cell-cycle checkpoints and DNA lesion-carryover into the M phase.

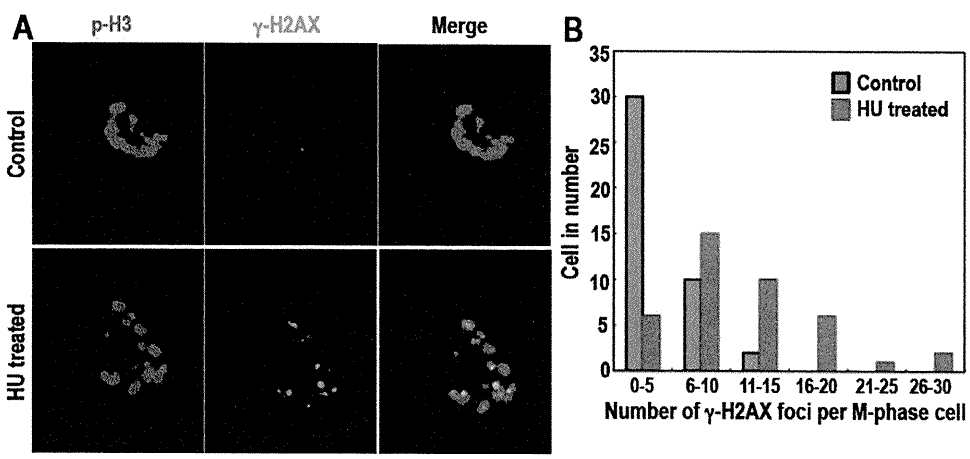

Figure 3. DNA lesions induced by replication stress are transmitted into the M phase. A,B. Using the normal human fibroblast SuSa, the carryover of DNA replication stress-associated lesions was determined after the transient treatment of 1 mM HU for 24 h and the subsequent nocodazole block as in Methods. The representative images (**A**) and the number of γH2AX foci per cell (**B**) are shown. The number of γH2AX foci was counted from 42 control cells and 40 replication stress-induced cells.
doi:10.1371/journal.pone.0008821.g003

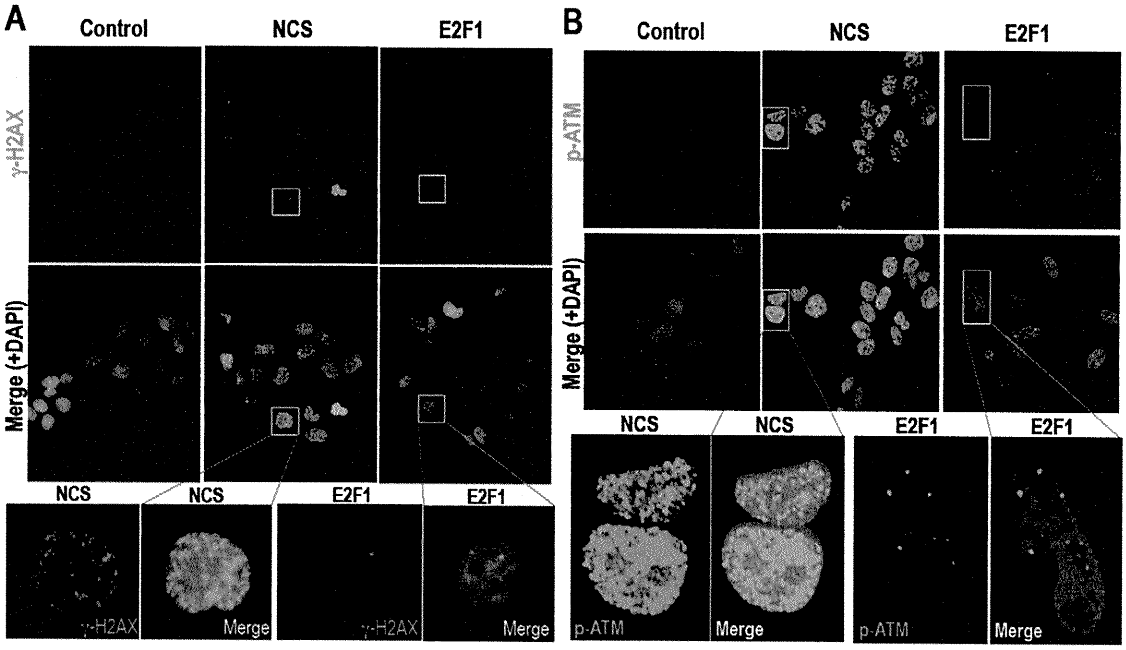

Figure 4. DNA replication stress causes only a small number of DNA lesions with limited ATM activation. A,B. Comparing cells activated with E2F1 as in Fig. 1A and cells damaged with 100 ng/ml NCS that causes G2-phase arrest, the statuses of DNA lesions and the resulting damage checkpoint activation were determined with γH2AX foci (**A**) and phosphorylated ATM (P-ATM) foci (**B**), respectively.
doi:10.1371/journal.pone.0008821.g004

DNA Lesions in the M Phase Cause Cytokinesis Failure

Another question remains: How do mitotic cells readily respond to DNA lesions that are carried over into the M phase? Despite the numerous studies on DNA damage response, only a few studies of those have been reported for the mitotic cells, showing M-phase specific DNA damage checkpoints [13,14]. Interestingly, one of these has reported tetraploidization with ionizing radiation in prometaphase HeLa cells [13]. Here, we found that such tetraploidization is a common phenomenon, independent of damaging sources (Fig. 5A) and cell types, including U2OS, WI-38, and MEFs (Supplementary Fig. S3), as long as cells existed in the M phase (Supplementary Fig. S4). These showed completely different responses to DNA damage in the M phase.

For the detailed study on tetraploidization with DNA lesions in mitotic cells, we used time-lapse imaging (Fig. 5B; Supplementary Movies S1, S2, S3, S4) and found that the damaged cells failed to complete cytokinesis and subsequently developed tetraploidy (Fig. 5B lower panels between 4:30 and 5:00). Importantly, such a cytokinesis failure was observed in the majority of cells (Supplementary Movie S4; Fig. 5A), and those still replicated DNA (Supplementary Fig. S5). Furthermore, despite the activation of DNA damage checkpoint proteins, including H2AX, ATM and Chk2 (Fig. 5C; Supplementary Fig. S6), damaged M-phase cells still exited from the mitotic phase and entered into the G1 phase, based on monitoring cyclins B and E as M- and G1-phase markers, respectively (Fig. 5D), indicating the dysfunctional DNA damage checkpoint during mitosis. Since cells had already exited from the metaphase, the spindle assembly checkpoint could not be responsible for DNA damage. In fact, a spindle assembly checkpoint factor, BubR1, exhibited normally (Supplementary Fig. S7). Thus, DNA damage checkpoints are not fully functional during mitosis, even if they exist [13,14].

In addition, tetraploidization was also observed in metaphase cells but was significantly lowered 15 min after metaphase release (Fig. 6A), suggesting the involvement of chromosome segregation, because chromosome segregation starts at the onset of the anaphase. In fact, the cells damaged in the prometaphase showed incomplete chromosome segregation (Fig. 6B). Furthermore, such chromosomal mis-segregation disrupted the spindle midzone structure, including Aurora-B localization (Fig. 6C), which is the essential conformation for cytokinesis [15,16]. Here, Aurora-B kinase was still active (Fig. 6D), though. A recent study has shown that Aurora-B functions to protect tetraploidization as an abscission checkpoint, although this is not the perfect block, either [11]. Taken together, these findings indicate that DNA lesions in the M phase cause a chromosome bridge and disrupt the spindle midzone structure, risking cytokinesis failure and tetraploidization.

MEFs Are Immortalized with Tetraploidy

As described above, DNA lesions induced by oncogenes, which could act as precancerous DNA lesions, are possibly carried over into the M phase, causing a chromosome-bridge and the resulting cytokinesis failure with tetraploidy generation. To confirm whether such scenario is really the case during spontaneous cell immortalization, we tested during the process of MEF-immortalization, (1) because MEFs are immortalized with the mutation in the Arf/p53 module similar to cancer development [17], (2) because primary MEFs often develop tetraploidy prior to immortalization, and (3) because senescing cells are known to spontaneously accumulate unrepairable DNA lesions [18], as potentially precancerous DNA lesions. We cultured growing-MEFs under the 3T3 protocol [19] and maintained senescing-MEFs with medium change (Fig. 7A). As well established, MEFs initially showed primary growth and then slowed down during senescene, which was followed by development of immortality. Intriguingly, all immortalized MEFs at early steps (IP2) were completely tetraploidy (Fig. 7B), implying that tetraploidization is the key step for MEF-immortalization. In addition, these immortalized MEFs lost the function of p53 accumulation in response to DNA damage, whereas senescing MEFs as well as

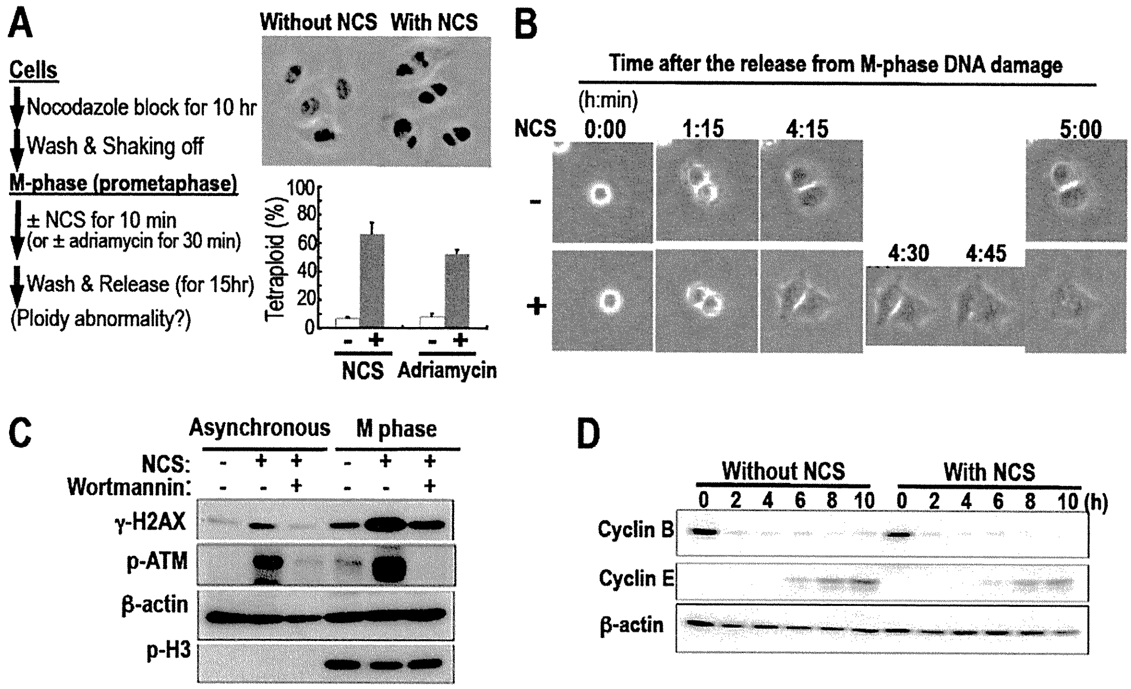

Figure 5. Damaged mitotic cells still proceed into cytokinesis with failure, resulting in tetraploidy generation. A. The tetraploidy generation was determined as in the scheme with DNA damage in the M phase. The fraction of tetraploidy was quantified from at least 100 cells in each of 3 independent experiments. Error bars in the graphs represent ± SD. **B.** Time-lapse imaging analyses were performed for the damaged cells as in **A** after the release. The representative images are displayed at the indicated time points. These results are also shown with movies [Supplementary movies S1, S3 (control) and S2, S4 (damaged with NCS)]. **C.** Mitotic cells still show the functional activation of DNA damage checkpoint factors, although cells still proceed into the G1 phase as in **D**. When indicated, the cells were incubated with 40 μM wortmannin for 1 h before NCS treatment. **D.** M-phase exit and G1-phase entry of the damaged cells as in **A** were determined with cyclins B and E as M- and G1-phase markers, respectively, after the release.
doi:10.1371/journal.pone.0008821.g005

primary growing MEFs showed p53 accumulation after DNA damage (Supplementary Fig. S8). This suggests that the induction of mutations is also associated with genomic instability development during immortality acquirement, although it is still unclear how the mutations are induced.

Spontaneous MEF-Tetraploidization Is Associated with M-Phase DNA Lesions and Chromosome-Bridge

To determine the possible association between M-phase DNA lesions and tetraploidy generation during MEF-imortalization, we examined the status of DNA lesions in the M-phase cells in each stage during the lifecycle of MEFs (Fig. 7C). Importantly, DNA-lesions in the mitotic cells were observed in the rarely growing senescent (M4 and M6) as well as in immortalized MEFs (IP32), but not in MEFs under primary growth (P4) or early senescence (M2) (Fig. 7C). These results indicate that spontaneous DNA lesions in the M phase starts to appear in the rarely growing senescent MEFs prior to the acquirement of immortality. Importantly, M-phase DNA lesions at M4 concurrently appeared with chromosome-bridge (Fig. 7D) and bi-nuclear tetraploidy (Fig. 7E). These results support that DNA lesions trigger the chromosome-bridge and the resulting tetraploidy generation during MEF-immortalization, because the observed bi-nuclear tetraploidy is a primary and transient status right after the development until the following M phase, in which daughter chromosomes assemble in a common metaphase plate to lead into tetraploidy with a single nucleus in the subsequent G1 phase [11]. Importantly, these results indicate that tetraploidy-generation associated with mitotic DNA-lesions is also the case during MEF immortalization. Furthermore, the resulting immortal MEFs (IP2) were totally tetraploidy (Fig. 7B), indicating that the tetraploidization step is critical for acquiring immortality. In addition, DNA lesions spontaneously accumulating in senescing cells act qualitatively similar to the lesions induced by oncogenes.

After immortalization, MEFs were mostly γH2AX-positive and continuously showed DNA lesions during mitosis (Fig. 7C), suggesting continuous genomic alterations. In fact, the continuous culture of immortalized MEFs resulted in chromosomal loss, i.e., aneuploidy, at IP32 (Fig. 7B), which is an identical characteristic to cancer cells showing continuous chromosomal instability [1]. These results also support the previously proposed hypothesis, i.e., aneuploidy generation via the unstable tetraploidy [5,6]. However, these M-phase lesions in the immortalized MEFs did not trigger further polyploidy generation (Fig. 7B). Similarly, tetraploidy causes growth retardation and thereby never becomes major, although spontaneous development of tetraploidy is often observed during HeLa cell cultivation via chromosome bridges [11]. While tetraploidization with M phase-DNA lesion must be a key step for acquiring immortality, the impact of tetraploidization is likely to different once cells are immortalized. Nevertheless, our results suggest that, during senescing MEF immortalization, M phase-DNA lesions trigger spontaneous development of tetraploidy.

Tetraploidy Development in MEFs Is Accelerated by DNA Replication Stress

Through above study, we showed that DNA replication stress-associated lesions are transmitted into the M phase, that DNA lesions during mitosis cause tetraploidy generation, and that the

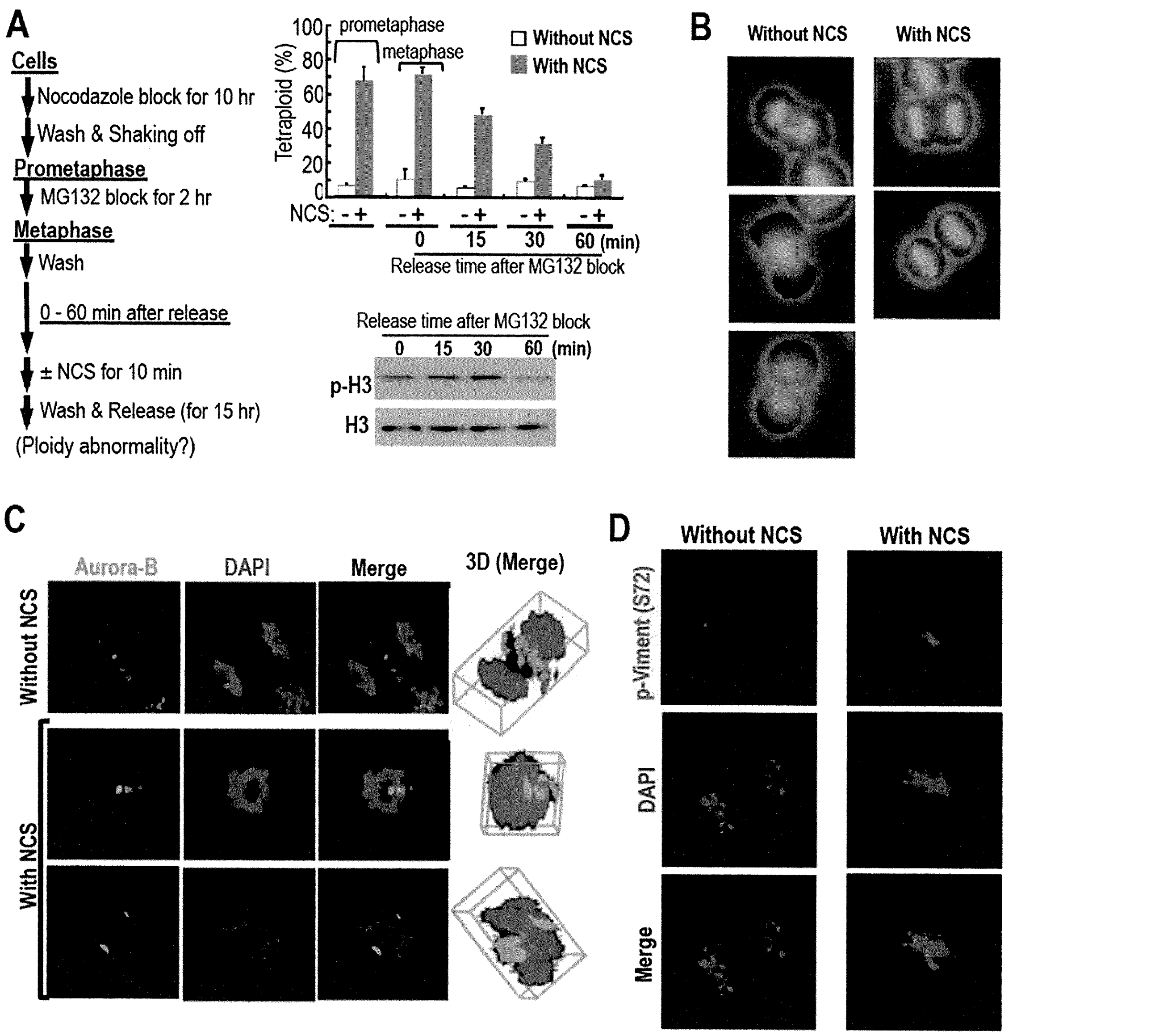

Figure 6. Mitotic DNA lesions cause chromosomal mis-segregation and a disruptive spindle mid-zone, followed by tetraploidy generation. **A.** DNA damage causes tetraploidy generation during metaphase but not after the onset of anaphase. The binuclear tetraploidy generation was assessed for the cells in metaphase or later as in the scheme using prometaphase cells prepared as in Figure 5A. Data were determined as in Figure 5A with at least 60 cells in each. **B.** To determine the chromosomal mis-segregation, cells damaged as in Figure 5A were released for 1 h and stained with DAPI. Images of the cells are at different mitotic stages. **C.** To determine the status of spindle midzone structure, cells damaged as in **A** were released for 1.5 h and analyzed for Aurora-B localization. Three-dimensional images are also displayed. **D.** Vimentin, a target of Aurola B, is activated with the phosphorylation status of vimentin at Ser 72 even under the chromosome mis-segregation, in which cells were treated with NCS for 1.5 h.
doi:10.1371/journal.pone.0008821.g006

identical processes are observed during the immortalization of MEFs. To directly confirm our original hypothesis (Supplementary Fig. S1), we further investigated whether tetraploidy generation could be directly induced by DNA replication stress in the pre-immortalizing MEFs (P3). Consistent with our above results, transient replication stress induced chromosome-bridge formation (Fig. 8A) and bi-nuclear tetraploidy accumulation (Fig. 8B,C) even in early passage MEFs (passage 3). Furthermore, these bi-nuclear tetraploidy MEFs were also subsequently immortalized. These indicate that DNA lesions induced by replication stress mediate tetraploidy generation in association with chromosome bridge formation during the acquirement of immortality.

Discussion

Cancer is a disease associated with genomic instability, which develops prior to tumor formation. Cells in the initial stages of cancer development exhibit precancerous DNA lesions and the competitive barrier responses [2,3]. Such stages are followed by the development of genomic instability [2,3], although it was elusive how and why genomic instability could develop in such situation. Our results showed one of the processes in developing genomic instability by precancerous DNA lesions, in which the lesions are carried over into the M phase and cause chromosomal mis-segregation and cytokinesis failure, resulting in tetraploidy generation. Such a conclusion is based on the following

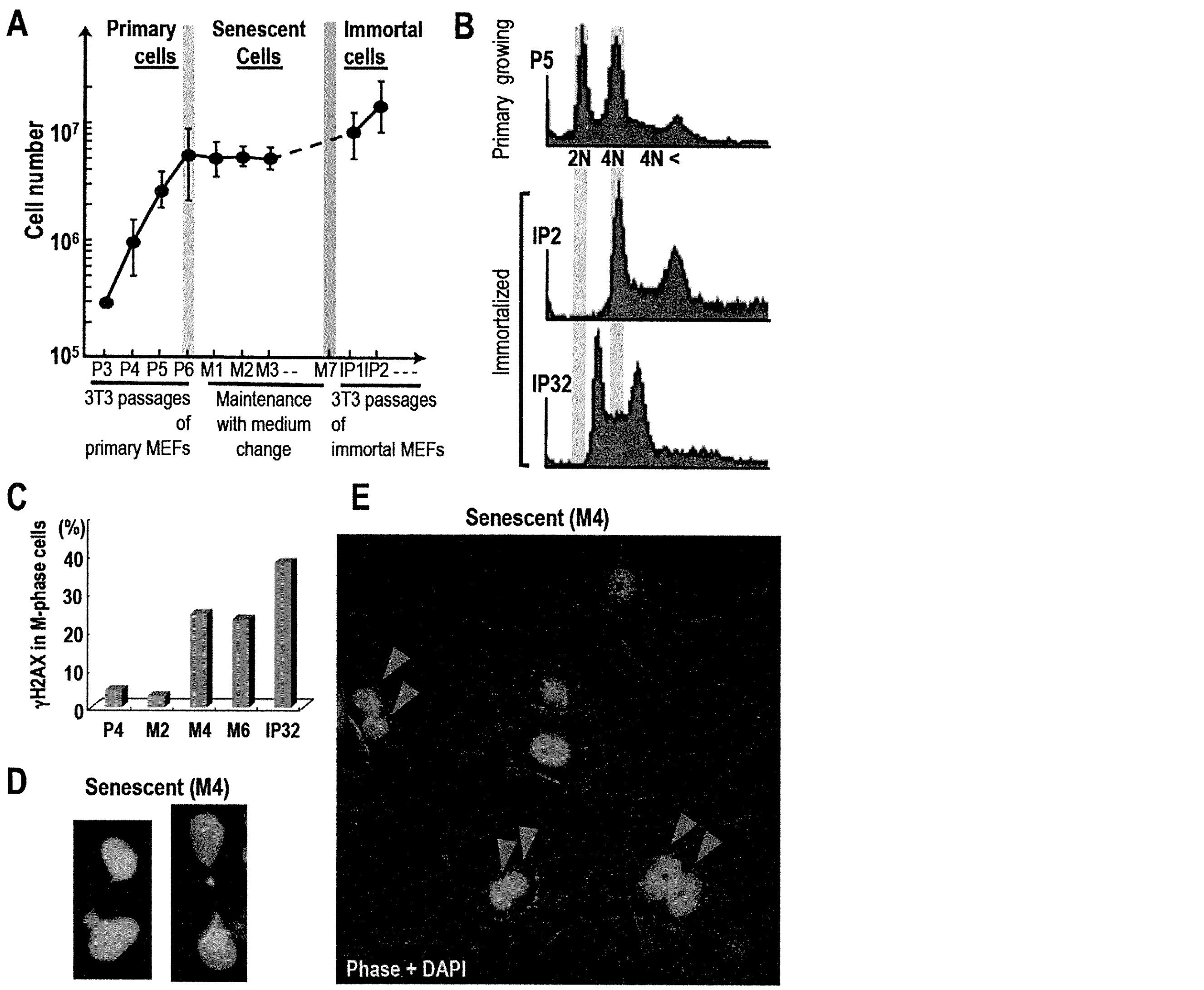

Figure 7. Senescing MEFs develop tetraploidy in association with mitotic DNA lesions and are accumulated with tetraploidy status before acquiring immortality. A. Growth curve of MEFs showed following 3 phases: primary growth (P3-P6); senescence (M1-M7); immortal growth (IP1-) phases. MEFs were passed under the 3T3 protocol or maintained with medium change once in 3 days. **B.** To determine the chromosomal status, either diploid or tetraploid/aneuploid, the chromosome contents were analyzed for primary growing (P5) and early (IP2) and late (IP32) immortalized MEFs. **C.** To determine the status of mitotic DNA lesions during the MEFs life cycle, MEFs in each step were determined by a double staining of γH2AX and phoshorylated H3 (p-H3) after nocodazole treatment (100 ng/ml, 12 h). γH2AX/p-H3 double positive fractions were determined at the indicated stages. **D.** Chromosome bridges were observed at M4. Images are representative. **E.** The image is representative at M4, showing the accumulation of cells with bi-nuclear tetraploidy. Arrowheads indicate cells with bi-nuclear tetraploid (Red arrowheads).
doi:10.1371/journal.pone.0008821.g007

mechanistic findings: DNA replication stress-associated lesions, which are induced by oncogene acceleration, can be carried over into the M phase; DNA lesions in mitotic cells cause chromosomal mis-segregation and the resulting cytokinesis failure.

Genomic instability is categorized in chromosomal instability (CIN) and microsatellite instability (MIN) [4]. While MIN is mostly characterized by mismatch repair (MMR) deficiency, CIN is usually MMR proficient. Our study revealed a process of CIN generation, especially tetraploidy/aneuploidy. Similarly, a previous study has shown that chromosomal translocation is also observed with G2-phase DNA lesions in the following G1 phase [20]. Thus, aberrant chromosomal segregation induced by DNA lesions might generally cause chromosomal alteration with the resulting loss of genomic homeostasis, which is also consistent with the observation of chromosomal loss in association with M-phase DNA lesions during the continuous culture of the immortalized MEFs (Fig. 7B).

Consistent with ageing-associated cancer-risk elevation, our results suggest that spontaneous DNA lesions accumulated in senescent cells during MEF immortalization act as precancerous DNA lesions, similar to the lesions induced by oncogene acceleration. Our results also show that DNA lesions generated by DNA replications stress are cryptogenic due to the limited impact on DNA lesions and the checkpoint activation, and that these lesions therefore induce genomic instability after the transmission into the M phase. Such a conclusion, i.e., genomic instability induction by DNA replication stress, is supported by the evidence of cancer predisposition with defective homologous recombination in BRCA1, BRCA2 and BLM helicase mutants [21–23], because DNA replication stress-associated lesions are primarily the target of homologous recombination.

Here we observed that the escape of G2/M checkpoint with DNA lesions triggers tetraploidy development. Contrary, previous

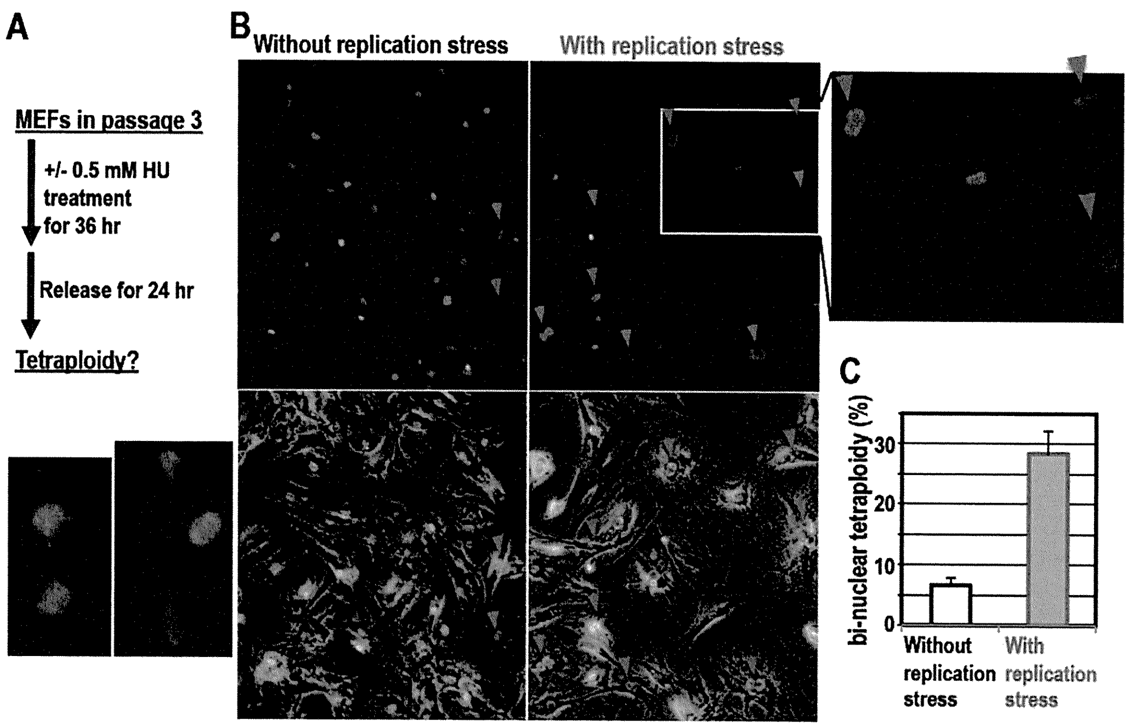

Figure 8. DNA replication stress induces chromosomal bridge formation and tetraploidy in early passage-primary MEFs. A. The effect of DNA replication stress was determined as in the scheme. After transient DNA replication stress, chromosome bridges were often observed. Representative images are shown. **B.** The images are representative with or without DNA replication stress. Arrowheads indicate cells with bi-nuclear tetraploid (red arrowheads). **C.** The proportions of total bi-nuclear cells were estimated. At least 100 cells were counted in each of 3 independent experiments.
doi:10.1371/journal.pone.0008821.g008

reports showed that the identical escape of G2/M checkpoint results in the mitotic catastrophe cell death [24–27]. How the identical DNA lesions could induce completely different effects? Although the mechanistic discrimination is unclear, so far the differences underlie if the cells are in immortal or pre-immortal. In cancer cells, cells with aneuploidy were accumulated after G2/M checkpoint-escape and after the appearance of chromosome bridge (Fig. 1,2). But such aneuploidy accumulates transiently and never come up to major, which was also shown in a previous HeLa cell study [11]. Such transient accumulation of aneuploidy coincided with the increase in sub-G1 fraction (Fig. 2B), suggesting the eventual death induction. In contrast, pre-immortal senescing cells are accumulated with bi-nuclear tetraploidy in association with the escape of G2/M checkpoint, and eventually acquire the immortality, which are totally tetraploidy. In fact, mitotic catastrophe-associated death induction has been mainly studied with the immortalized cells mostly in cancer cell lines, which are described as a goal of cancer therapies. Contrary, somehow pre-immortal cells are resistant to the identical DNA lesions and survive, contributing the development of the immortality.

Prior to acquiring immortality, senescing MEFs are accumulated with a bi-nuclear phenotype that is a primary and transient form of tetraploidy, indicating that such tetraploidy generation in senescing cells is the major event in these stages in association with M-phase DNA lesions, aberrancy in chromosomal segregation and cytokinesis failure. Since immortalized MEFs are totally tetraploidy, these steps must be critical for immortalization. It has been shown that immortalized MEFs are mutated in the Arf/p53 module [17]. We also observed that the Arf/p53 module responds normally in senescing MEFs unlike that in immortalized MEFs (Supplementary Fig. S8), suggesting that the selective pressure of mutants is also coupled with acquiring immortality and tetraploidy development. Here we showed the mechanistic steps of MEFs immortalization, which share with the process of cancer development in many aspects. However, unlike MEFs, primary human cells usually do not show such spontaneous transformation. Difference in MEFs and human cells is mainly because MEFs express TERT and suffer from accelerated growth stimulation with 10% fetal bovine serum, whereas primary human cells require hTERT and the additional acceleration of oncogenes such as Myc, Ras etc. for the immortalization [28,29]. Importantly, our results suggest that the trigger for immortality acquirement-associated development of genomic instability is the precancerous DNA replication stress with oncogene acceleration or with senescence-associated repair deficiency with continuous growth stimulation.

Materials and Methods

Cell Culture, Oncogene Induction, Cell Synchronization, Cell Damage and Replication Stress Induction

Cancer cell lines and normal human fibroblast SuSa were cultured as previously described [30]. MEF cells were prepared as previously described [19]. MEFs were cultured under 3T3 passage protocol [19], in which 3×10^5 MEFs were passed in 6-cm dishes every 3 days using 10% fetal bovine serum containing DMEM (during P1-P6 and after IP1), otherwise maintained with medium-change under the same medium conditions every 3 days (during M1-M7). ER-E2F1 expressing U2OS cells were treated with 4-hydroxytamoxifen (300 nM) as previously described [31]. For transient expression of *Cdc25A*, *Cdc25A* cDNA was inserted into pIREShyg2 vector (Clontech Laboratories, Palo Alto, CA). The

Cdc25A expression vector, empty vector, or none was then transfected into HEK293 cells with FuGENE6. Prometaphase cells were prepared as previously reported [32]. For the preparation of metaphase cells, prometaphase cells were further incubated with 10 μM MG132 for 2 h [33]. These synchronization and chromosome contents were determined with flow cytometry as previously described [32]. DNA double-strand breaks were directly induced by 100 ng/ml NCS (Pola Pharma, Tokyo, Japan) for 10 min or by 2.5 μM adriamycin for 1 h. Induced DNA lesions were detected by γH2AX, which were confirmed with comet assay after NCS treatment (Supplementary Fig. S9). For DNA replication stress-associated DNA-LCM study, SuSa cells were transiently treated with 1 mM HU for 24 h and then released in 10 % FBS DMEM with 20 ng/ml nocodazole for 10 h.

Antibodies, Immunostaining and Western Blotting

Antibodies against γH2AX (JBW301, Upstate Biotechnology) and phospho-histone H3 (Ser 10) (Upstate Biotechnology) were used for immnostaining and Western blot analysis. Antibodies against phospho-ATM (Ser 1981) (10H11.E12, Cell Signaling Technology), phospho-Chk2 (Thr 68) (Cell Signaling Technology), β-actin (AC-74, Sigma), histone H3 (ab1791, Abcam), cyclin B1 (GNS1, Santa Cruz Biotechnology Inc.), p53 (Pab240, Santa Cruz Biotechnology Inc.) and cyclin E (Ab-1, Calbiochem) were used for Western blot analysis. Antibodies against AIM-1 (Aurora-B) (BD Transduction Laboratories), phospho-vimentin (Ser 72) [34], BubR1 (8G1, Upstate Biotechnology) and phospho-ATM (Ser 1981) (clone 7C10D8, Rockland) were used for immunostaining. Before immunostaining with primary and secondary antibodies, cells were fixed with 4% paraformaldehyde for 10 min and permeabilized with 0.1% Triton X-100/PBS for 10 min. For confocal microscope imaging, cells were cultured on coverslips and stained as above. Other immunofluorescence images were captured with ECLIPSE TE300 inverted microscope (Nikon) or LSM510 confocal microscope (Carl Zeiss). Three-dimensional images were constructed with 1 μm-slice pictures of the cells using LSM Image Browser software. Western blot analysis was performed as previously described [32].

Immunofluorescence and Time-Lapse Imaging

Fifteen hours after the release from M phase-DNA damage, cells were fixed with 10% neutral buffered formalin for 10 min, permeabilized with 0.3% Triton X-100/PBS for 10 min, and stained with DAPI for 5 min. Phase contrast images merged with immunofluorescence images were captured with ECLIPSE TE300 inverted microscope. Time-lapse images were acquired with Multicell-imaging incubator (Sanyo).

Comet Assay

A comet assay was performed as previously described [32].

Chromosome Spreads

Mitotic cells were prepared in a 6-h treatment with 20 ng/ml nocodazole and shaking-off. The collected cells were hypotonically swollen with 75 mM KCl for 15 min, and then fixed with −20°C Carnoy's solution (75% methanol/25% acetic acid) for 20 min. The fixative was changed once and the cells in Carnoy's solution were dropped onto glass slides and air-dried. The slides were stained with 4% Giemsa (Merck) solution for 10 min, washed briefly in tap water, and air-dried.

Supporting Information

Movie S1 Movies S1-S4. For the precise investigation of the process of tetraploidy development in the M-phase cells with DNA lesions, time-lapse imaging was performed. After cells were damaged with NCS as in Fig. 5A, the damaged cells (Movies S2 and S4) or non-damaged control (Movies S1 and S3) were monitored with close-up views (Movies S1 and S2) or wide-range views (Movies S3 and S4). The images shown in Fig. 5B are from those in Movies S1 and S2.
Found at: doi:10.1371/journal.pone.0008821.s001 (0.27 MB MOV)

Movie S2 Movies S1-S4. For the precise investigation of the process of tetraploidy development in the M-phase cells with DNA lesions, time-lapse imaging was performed. After cells were damaged with NCS as in Fig. 5A, the damaged cells (Movies S2 and S4) or non-damaged control (Movies S1 and S3) were monitored with close-up views (Movies S1 and S2) or wide-range views (Movies S3 and S4). The images shown in Fig. 5B are from those in Movies S1 and S2.
Found at: doi:10.1371/journal.pone.0008821.s002 (0.27 MB MOV)

Movie S3 Movies S1-S4. For the precise investigation of the process of tetraploidy development in the M-phase cells with DNA lesions, time-lapse imaging was performed. After cells were damaged with NCS as in Fig. 5A, the damaged cells (Movies S2 and S4) or non-damaged control (Movies S1 and S3) were monitored with close-up views (Movies S1 and S2) or wide-range views (Movies S3 and S4). The images shown in Fig. 5B are from those in Movies S1 and S2.
Found at: doi:10.1371/journal.pone.0008821.s003 (1.41 MB MOV)

Movie S4 Movies S1-S4. For the precise investigation of the process of tetraploidy development in the M-phase cells with DNA lesions, time-lapse imaging was performed. After cells were damaged with NCS as in Fig. 5A, the damaged cells (Movies S2 and S4) or non-damaged control (Movies S1 and S3) were monitored with close-up views (Movies S1 and S2) or wide-range views (Movies S3 and S4). The images shown in Fig. 5B are from those in Movies S1 and S2.
Found at: doi:10.1371/journal.pone.0008821.s004 (1.09 MB MOV)

Figure S1 Hypothesis. Cells damaged with precancerous DNA lesions develop tetraploidy hypothetically via chromosomal bridges during chromosomal segregation (bottom), unlike cell division in cells without DNA lesions (top). If this is the case, generated cells with tetraploidy are primarily and transiently bi-nuclear until the following M phase, in which daughter chromosomes assemble in a common metaphase plate to lead into tetraploidy with a single nucleus in the subsequent G1 phase.
Found at: doi:10.1371/journal.pone.0008821.s005 (3.03 MB TIF)

Figure S2 Transient over-expression of Cdc25A promotes DNA lesions including the cells during mitosis. Empty (control) or Cdc25A expression (Cdc25A) vectors were transfected into HEK293 cells. After cultivation for two days, cells were determined with the indicated antibodies.
Found at: doi:10.1371/journal.pone.0008821.s006 (3.02 MB TIF)

Figure S3 Tetraploidy generation with DNA damage during mitosis in U2OS, WI-38 and primary MEFs. A. Cells prepared as in the experimental scheme on Fig. 5A were stained with DAPI. The arrowheads indicate bi-nuclear tetraploid cells. B. Quantification of the tetraploid cells was performed with at least 100 cells for each.
Found at: doi:10.1371/journal.pone.0008821.s007 (2.99 MB TIF)

Figure S4 Cells damaged during mitosis lead to tetraploidy generation but not during interphase. HeLa cells in the M phase or without synchronization were treated as in the scheme. Unlike

asynchronous cells, M phase-cells specifically develop tetraploidy after damage. Quantification of the tetraploid cells was performed with at least 100 cells for each.
Found at: doi:10.1371/journal.pone.0008821.s008 (2.21 MB TIF)

Figure S5 The cells damaged in the M phase further replicate DNAs in the following S phase. A,B. After cells were damaged with NCS (A) or adriamycin (B) as in Fig. 5A, the chromosome contents of the cells after the release were analyzed by flow cytometry.
Found at: doi:10.1371/journal.pone.0008821.s009 (1.10 MB TIF)

Figure S6 DNA damage checkpoint activation is durable in the M phase, but dysfunctional to induce arrest during mitosis. The activation of DNA damage checkpoint protein Chk2 in the HeLa asynchronous and M-phase cells characterized by phosphorylated histone H3 (P-H3) was analyzed for the phosphorylated form.
Found at: doi:10.1371/journal.pone.0008821.s010 (0.37 MB TIF)

Figure S7 Prometaphase-DNA damage does not affect the behavior of BubR1 and the progression into the anaphase and the telophase. At 75 min after the release from NCS treatment as in the experimental scheme on Fig. 5A, the cells were stained with anti-BubR1 antibody and DAPI. For the NCS-treated cells, the mitotic stages in the anaphase and the telophase are estimated based on the degree of cell elongation.
Found at: doi:10.1371/journal.pone.0008821.s011 (4.78 MB TIF)

Figure S8 Arf/p53 module mutation in the immortalized MEFs. To determine the loss of Arf/p53 module, p53 accumulation was monitored 12 h after 100 ng/ml NCS treatment at each stage of MEFs: primary growth (P4); senescence (M2); immortalized (IP2).
Found at: doi:10.1371/journal.pone.0008821.s012 (0.63 MB TIF)

Figure S9 DNA lesions indicated by γH2AX were also confirmed with comet assay. DNA lesions, indicated by γH2AX in this study, were also confirmed by comet assay with the tails after NCS treatment for 15 min. Arrow heads indicate the spots with comet tails, indicating DNA damages.
Found at: doi:10.1371/journal.pone.0008821.s013 (2.88 MB TIF)

Acknowledgments

We thank K Helin for kindly providing ER-E2F1-expressing U2OS cells.

Author Contributions

Conceived and designed the experiments: YI KiY. Performed the experiments: YI KiY YY KS HF JU. Analyzed the data: KiY MT HG MI SM HT. Contributed reagents/materials/analysis tools: MT HG MI. Wrote the paper: KiY HT.

References

1. Lengauer C, Kinzler KW, Volgelstein B (1997) Genetic instability in colorectal cancers. Nature 386: 623–627.
2. Bartkova J, Horejsi Z, Koed K, Krämer A, Tort F, et al. (2005) DNA damage response as a candidate anti-cancer barrier in early human tumorigenesis. Nature 434: 864–870.
3. Gorgoulis VG, Vassiliou LV, Karakaidos P, Zacharatos P, Kotsinas A, et al. (2005) Activation of the DNA damage checkpoint and genomic instability in human precancerous lesions. Nature 434: 907–913.
4. Lengauer C, Kinzler KW, Vogelstein B (1998) Genetic instabilities in human cancers. Nature 396: 643–649.
5. Ganem NJ, Storchova Z, Pellman D (2007) Tetraploidy, aneuploidy and cancer. Curr Opin Genet Dev 17: 157–162.
6. Shi Q, King RW (2005) Chromosome nondisjunction yields tetraploid rather than aneuploid cells in human cell lines. Nature 437: 1038–1042.
7. Fujiwara T, Bandi M, Nitta M, Ivanova EV, Bronson RT, et al. (2005) Cytokinesis failure generating tetraploids promotes tumorigenesis in p53-null cells. Nature 437: 1043–1047.
8. Musacchio A, Salmon ED (2007) The spindle-assembly checkpoint in space and time. Nat Rev Mol Cell Biol 8: 379–393.
9. Weaver BA, Silk AD, Montagna C, Verdier-Pinard P, Cleveland DW (2007) Aneuploidy acts both oncogenically and as a tumor suppressor. Cancer Cell 11: 25–36.
10. Sotillo R, Hernando E, Díaz-Rodríguez E, Teruya-Feldstein J, Cordón-Cardo C, et al. (2007) Mad2 overexpression promotes aneuploidy and tumorigenesis in mice. Cancer Cell 11: 9–23.
11. Steigemann P, Wurzenberger C, Schmitz MHA, Held M, Guizetti J, et al. (2009) Aurora B-mediated abscission checkpoint protects against tetraploidization. Cell 136: 473–484.
12. Deckbar D, Birraux J, Krempler A, Tchouandong L, Beucher A, et al. (2007) Chromosome breakage after G2 checkpoint release. J Cell Biol 176: 749–755.
13. Huang X, Tran T, Zhang L, Hatcher R, Zhang P (2005) DNA damage-induced mitotic catastrophe is mediated by the Chk1-dependent mitotic exit DNA damage checkpoint. Proc Nat Acad Sci USA 102: 1065–1070.
14. Mikhailov A, Cole RW, Rieder CL (2002) DNA damage during mitosis in human cells delays the metaphase/anaphase transition via the spindle-assembly checkpoint. Curr Biol 12: 1797–1806.
15. Carmena M, Earnshaw WC (2003) The cellular geography of aurora kinases. Nat Rev Mol Cell Biol 4: 842–854.
16. McCollum D (2004) Cytokinesis: the central spindle takes center stage. Curr Biol 14: R953–R955.
17. Matheu A, Maraver A, Klatt P, Flores I, Garcia-Cao I, et al. (2007) Delayed ageing through damage protection by the Arf/p53 pathway. Nature 448: 375–379.
18. Sedelnikova OA, Horikawa I, Zimonjic DB, Popescu NC, Bonner WM, et al. (2004) Senescing human cells and ageing mice accumulate DNA lesions with unrepairable double-strand breaks. Nature Cell Biol 6: 168–170.
19. Todaro GJ, Green H (1963) Quantitative studies of the growth of mouse embryo cells in culture and their development into established lines. J Cell Biol 17: 299–313.
20. Nakada S, Katsuki Y, Imoto I, Yokoyama T, Nagasawa M, et al. (2006) Early G2/M checkpoint failure as a molecular mechanism underlying etoposide-induced chromosomal aberrations. J Clin Invest 116: 80–89.
21. Scully R, Livingston DM (2000) In search of the tumour-suppressor functions of BRCA1 and BRCA2. Nature 408: 429–432.
22. Powell SN, Kachnic LA (2003) Roles of BRCA1 and BRCA2 in homologous recombination, DNA replication fidelity and the cellular response to ionizing radiation. Oncogene 22: 5784–5791.
23. Tripathi V, Nagarjuna T, Sengupta S (2007) BLM helicase-dependent and -independent roles of 53BP1 during replication stress-mediated homologous recombination. J Cell Biol 178: 9–14.
24. Chan TA, Hermeking H, Lengauer C, Kinzler KW, Vogelstein B (1999) 14-3-3σ is required to prevent mitotic catastrophe after DNA damage. Nature 401: 616–620.
25. Roninson IB, Broude EV, Chang BD (2001) If not apoptosis, then what? Treatment-induced senescence and mitotic catastrophe in tumor cells. Drug Resist. Update 4: 303–313.
26. Nitta M, Kobayashi O, Honda S, Hirota T, Kuninaka S, et al. (2004) Spindle checkpoint function is required for mitotic catastrophe induced by DNA-damaging agents. Oncogene 23: 6548–6558.
27. Reinhardt HC, Aslanian AS, Lees JA, Yaffe MB (2007) p53-deficient cells rely on ATM- and ATR-mediated checkpoint signaling through the p38MAPK/MK2 pathway for survival after DNA damage. Cancer Cell 11: 175–189.
28. Narisawa-Saito M, Handa K, Yugawa T, Ohno S, Fujita M, et al. (2007) HPV16 E6-mediated stabilization of ErbB2 in neoplastic transformation of human cervical keratinocytes. Oncogene 26: 2988–2996.
29. Sasaki R, Narisawa-Saito M, Yugawa T, Fujita M, Tashiro H, et al. (2009) Oncogenic transformation of human ovarian surface epithelial cells with defined cellular oncogenes. Calcinogenesis 30: 423–431.
30. Yoshioka K, Yoshioka Y, Hsieh P (2006) ATR kinase activation mediated by MutSα and MutLα in response to cytotoxic O^6-methylguanine adducts. Mol Cell 22: 501–510.
31. Müller H, Bracken AP, Vernell R, Moroni MC, Christians F, et al. (2001) E2Fs regulate the expression of genes involved in differentiation, development, proliferation, and apoptosis. Genes Dev 15: 267–285.
32. Ichijima Y, Sakasai R, Okita N, Asahina K, Mizutani S, et al. (2005) Phosphorylation of histone H2AX at M phase in human cells without DNA damage response. Biochem Biophys Res Commun 336: 807–812.
33. Petronczki M, Glotzer M, Kraut N, Peters JM (2007) Polo-like kinase 1 triggers the initiation of cytokinesis in human cells by promoting recruitment of the RhoGEF Ect2 to the central spindle. Dev Cell 12: 713–725.
34. Goto H, Yasui Y, Kawajiri A, Nigg EA, Terada Y, et al. (2003) Aurora-B regulates the cleavage furrow-specific vimentin phosphorylation in the cytokinetic process. J Biol Chem 278: 8526–8530.

ELSEVIER

Brain & Development 32 (2010) 685–687

BRAIN & DEVELOPMENT
Official Journal of the Japanese Society of Child Neurology

www.elsevier.com/locate/braindev

Case report

Low-dose levodopa is effective for laryngeal dystonia in xeroderma pigmentosum group A

Rie Miyata [a,*], Toru Sasaki [b], Masaharu Hayashi [c], Satoshi Araki [d], Masayuki Shimohira [d], Jun Kohyama [a]

[a] *Department of Pediatrics, Tokyo Kita Shakai Hoken Hospital, 4-17-56 Akabanedai, Kita-ku, Tokyo 115-0053, Japan*
[b] *Department of Otorhinolaryngology, Tokyo Kita Shakai Hoken Hospital, 4-17-56 Akabanedai, Kita-ku, Tokyo 115-0053, Japan*
[c] *Department of Clinical Neuropathology, Tokyo Metropolitan Institute for Neuroscience, Tokyo, Japan*
[d] *Department of Pediatrics, Tokyo Medical and Dental University, Tokyo, Japan*

Received 3 June 2009; received in revised form 9 September 2009; accepted 9 September 2009

Abstract

Xeroderma pigmentosum (XP), a genetic disorder in DNA nucleotide excision repair, is characterized by skin hypersensitivity to sunlight and progressive neurological impairment. Laryngeal dystonia and vocal cord paralysis are complications that can arise in older XP group A (XPA) patients. We report three patients with XPA being administered low-dose levodopa (0.3–1.5 mg/kg/day) for laryngeal dystonia. Patients were aged from 13 to 18 years, exhibited paroxysmal choking and inspiratory stridor, and were diagnosed with laryngeal dystonia. Two XPA patients responded to low-dose levodopa, and paroxysmal choking and involuntary movements resolved, although one of the two patients showed incomplete resolution due to suspected vocal cord paralysis. The other patient was unable to tolerate the medication because of a transient decrease of muscle tone in the extremities. We previously reported a decreased immunostaining of dopaminergic (DA) terminals in the basal ganglia of XPA patients, which may be involved in laryngeal dystonia. Low-dose levodopa has been reported to alleviate DA receptor supersensitivity in tic patients, while laryngeal dystonia occurs in patients with tardive dyskinesia caused by DA receptor supersensitivity. Thus, low-dose levodopa may improve laryngeal dystonia by alleviating DA receptor supersensitivity in XPA patients. We recommend that low-dose levodopa be used for treatment of paroxysmal respiratory disturbances and/or involuntary movements in XPA patients.

Keywords: Xeroderma pigmentosum; Laryngeal dystonia; Levodopa; Dopamine; Basal ganglia

1. Introduction

Xeroderma pigmentosum (XP), a genetic disorder in DNA nucleotide excision repair, is characterized by skin hypersensitivity to sunlight and progressive neurological impairment [1]. The common complementation subgroup of XP in Japan is group A (XPA). XPA leads to severe neurological disorders including mental deterioration, cerebellar ataxia, extrapyramidal abnormalities, and neuronal deafness; however, there are no effective treatments for such symptoms [2]. Laryngeal dystonia is characterized by paroxysmal stridor due to vocal cord dystonia, and is observed in extrapyramidal disorders [3]. Laryngeal dystonia and vocal cord paralysis are complications that can arise in older XPA patients and can be life threatening [4,5]. We previously demonstrated selective damage to the dopamine (DA) neurons in the substantia nigra of XPA cases at autopsy [6]. Herein, we report three patients with clinically or genetically confirmed XPA who received low-dose levodopa for laryngeal dystonia. In two of the three patients, laryngeal dystonia and involuntary movements in the

* Corresponding author. Tel.: +81 3 5963 3311; fax: +81 3 5963 6678.
E-mail address: rie88miyata@ybb.ne.jp (R. Miyata).

0387-7604/$ - see front matter
doi:10.1016/j.braindev.2009.09.008

upper extremities were relieved. Parental consent in addition to the approval of the chief of the hospital ethical committee was obtained for all cases.

2. Case report

Patient 1 was an XPA female aged 18 years and 8 months with a homozygous splicing mutation in intron 3. She began using a hearing aid for neuronal deafness at 8 years, she developed rigidity in the extremities in her teens, and had received anticonvulsants since she was 13 years. Brain MRI demonstrated diffuse atrophy in the cerebrum, cerebellum, and brainstem. At 16 years, she began to show dysphagia and myoclonic movements during wakefulness in the upper extremities, and started medication for a neurogenic bladder. A surface electromyogram was not performed. She developed nighttime inspiratory stridor, and laryngoscopy (LS) was performed at 17 years. On LS, vocal cord movement was restricted, and the glottis tended to be fixed in the midline during inspiratory and expiratory phases (Fig. 1A), although no morphological abnormalities were found in the arytenoid processes. She began to experience paroxysmal choking during meals and sleep at 17 years and 2 months, with subsequent LS revealing restricted movements in the vocal cord. We suspected that her symptoms were due to laryngeal dystonia, and started low-dose therapy of levodopa (0.3 mg/kg/day) at 17 years and 10 months. Her nighttime inspiratory stridor, paroxysmal choking, and myoclonic movements of the upper extremities resolved, and LS showed a partial improvement in vocal cord opening (Fig. 1B). The patient developed transient, mild motor weakness in the extremities a few days after the start of levodopa, which disappeared spontaneously. She suffered from viral respiratory infection at 18 years and 1 month, during which nighttime inspiratory stridor reappeared, and the levodopa dose was increased to 0.6 mg/kg/day. Both inspiratory stridor and dysphagia then resolved, and vocal cord adduction and abduction were completely normalized on LS (Fig. 1C). The respiration and vocal cord movements on LS remain normal at 20 years.

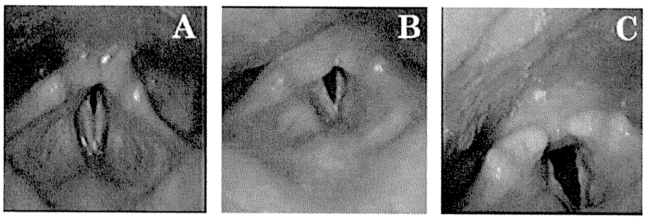

Fig. 1. Laryngoscopy findings during inspiratory phase in patient 1. (A) At 17 years of age, the glottis was fixed in the midline. (B) At 18 years of age, 3 months after the initiation of levodopa, the vocal cord showed restricted opening. (C) At 18 years of age, after the dose of levodopa was increased, the vocal cord showed normal opening.

Patient 2 was a male XPA patient aged 18 years and 10 months without genetic analysis. He developed rigidity in the extremities and hand tremors during wakefulness in his teens. A surface electromyogram was not performed. He first presented with inspiratory stridor after suffering respiratory infections at 12 years. Nighttime inspiratory stridor began when he was 13. Brain MRI was not performed due to severe dyspnea caused by the sedation. When he was 17, the patient developed paroxysmal choking during his meals and sleep, and awoke during his sleep due to dyspnea. On LS, vocal cord movements were restricted, the glottis tended to be fixed in the midline during inspiratory and expiratory phases, and there was mucosal swelling in the arytenoid processes. We diagnosed him with laryngeal dystonia, and he was treated with low-dose levodopa (0.3 mg/kg/day) beginning at 18 years and 2 months. Since neither inspiratory stridor during night nor the LS findings showed any changes, the dose of levodopa was increased to 0.6 mg/kg/day after 2 months. Inspiratory stridor at night, paroxysmal choking during his sleep, and hand tremors resolved, although choking during meals persisted. At 20, he is being treated with levodopa (1.5 mg/kg/day), and the dyspnea and abnormal movements of vocal cord on LS are gradually aggravating.

Patient 3 was an XPA male aged 13 years and 3 months with a homozygous splicing mutation in intron 3. He exhibited nighttime choking at 9 years. He developed mild rigidity in the lower extremities from the age of 10 years. At 12 years and 3 months, inspiratory stridor appeared occasionally during his meals, occurring suddenly in the absence of antecedent events. We diagnosed the patient with laryngeal dystonia, and he was treated with low-dose levodopa (0.5 mg/kg). Although he was able to walk independently before the initiation of levodopa, he began to frequently stagger and stumble. Levodopa was discontinued after 4 days at parental request. Limb weakness continued to aggravate, however, and he began to frequently drop objects and could not walk without support. He required a wheel chair for transfer and parental assistance during meals. It took 3 months for complete recovery of his motor abilities. Since he did not visit our hospital, the detailed neurological examination was not performed until the complete improvement of motor weakness. Neither brain MRI nor LS was performed.

3. Discussion

Laryngeal dystonia is caused by disturbed synergy of the laryngeal muscles during phonation or respiration [7]. Laryngeal electromyography is useful for the diagnosis of laryngeal dystonia, but was unable to be performed in our patients due to the risks and lack of consent. Botulinum toxin has been used for treatment of laryngeal dystonia in adults, while anticholinergics, benzodiazepines, dopamine-depleting agents, and baclofen have also been evaluated, although their efficacy is uncertain.

Expression of tyrosine hydroxylase in the nigrostriatal input, intrastriatal connections, and striatal outputs was previously shown to be impaired in XPA autopsy cases [6], and is likely to be involved in laryngeal dystonia [3]. In Tourette's syndrome, functional neuroimaging studies have suggested DA receptor supersensitivity in the basal ganglia, while low-dose levodopa can alleviate DA receptor supersensitivity and decrease tics in some patients [8]. The DA receptor supersensitivity in the basal ganglia caused by neuroleptics and antipsychotics can lead to tardive dyskinesia [9], and patients with tardive dyskinesia have been reported to suffer from laryngeal dystonia [10]. Speculatively, low-dose levodopa may ameliorate laryngeal dystonia by means of alleviating DA receptor supersensitivity in the basal ganglia in XPA patients. However, the mechanism of how low-dose levodopa alleviated myoclonus and tremor remains unclear.

In our patients, the paroxysmal event-specific occurrence of inspiratory stridor and choking strongly indicated laryngeal dystonia. However, patient 2 may have also suffered from vocal cord paralysis [5], as indicated by insufficient response to treatment. Patients 1 and 2 responded to low-dose levodopa with resolution of paroxysmal choking and involuntary movements, without serious adverse effects. Patient 3 showed decreased limb muscle tone and was unable to tolerate medication. Speculatively, levodopa may have moderated his muscle tone increase due to DA supersensitivity, and unmasked muscle hypotonia caused by a peripheral nerve lesion and cerebellar atrophy. Since motor weakness just after the start of levodopa was transient in patient 1, muscle hypotonia may have improved after a longer-term of levodopa.

We suggest that low-dose levodopa can be effective for intractable neurological disorders in XP patients, and recommend the introduction of low-dose levodopa, under close observation, for paroxysmal respiratory disturbances and/or involuntary movements.

Conflicts of interest

There are no conflicts of interest to declare.

References

[1] Kraemer KH, Patronas NJ, Schiffmann R, Brooks BP, Tamura D, Digiovanna JJ. Xeroderma pigmentosum, trichothiodystrophy and Cockayne syndrome: a complex genotype–phenotype relationship. Neuroscience 2007;145:1388–96.

[2] Nishigori C, Moriwaki S, Takebe H, Tanaka T, Imamura S. Gene alterations and clinical characteristics of xeroderma pigmentosum group A patients in Japan. Arch Dermatol 1994;130:191–7.

[3] Hamano K, Kumada S, Hayashi M, Naito R, Hayashida T, Uchiyama A, et al. Laryngeal dystonia in a case of severe motor and intellectual disabilities due to Japanese encephalitis sequelae. Brain Dev 2004;26:335–8.

[4] Muto H, Matsui A, Saito Y, Iwamoto H, Kaneko K, Masuko K, et al. Laryngeal dystonia in xeroderma pigmentosum. Brain Dev 2005;27:598–601.

[5] Ohto T, Iwasaki N, Okubo H, Shin K, Matsui A. Life-threatening vocal cord paralysis in a patient with group A xeroderma pigmentosum. Pediatr Neurol 2004;30:222–4.

[6] Hayashi M, Araki S, Kohyama J, Shioda K, Fukatsu R, Tamagawa K. Brainstem and basal ganglia lesions in xeroderma pigmentosum group A. J Neuropathol Exp Neurol 2004;63:1048–57.

[7] Grillone GA, Chan T. Laryngeal dystonia. Otolaryngol Clin North Am 2006;39:87–100.

[8] Nomura Y, Segawa M. Neurology of Tourette's syndrome (TS) TS as a developmental dopamine disorder: a hypothesis. Brain Dev 2003;25:S37–42.

[9] Margolese HC, Chouinard G, Kolivakis TT, Beauclair L, Miller R. Tardive dyskinesia in the era of typical and atypical antipsychotics. Part 1: Pathophysiology and mechanisms of induction. Can J Psychiatry 2005;50:541–7.

[10] Rowley H, Lynch T, Keogh I, Russell J. Tardive dystonia of the larynx in a quadriplegic patient: an unusual cause of stridor. J Laryngol Otol 2001;115:918–9.

VI.　毛細血管拡張性運動失調症ハンドブック

毛細血管拡張性運動失調症の治療法を研究する民間非営利団体です。

毛細血管拡張性運動失調症チルドレンズ・プロジェクト
CHILDREN'S PROJECT®

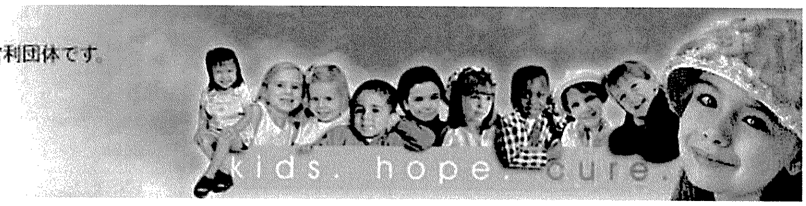

毛細血管拡張性運動失調症ハンドブック
Ataxia Telangiectasia Handbook

AT チルドレンズ・プロジェクト

AT Children' s project

平成 21-23 年度厚生労働科学研究費補助金(難治性疾患克服研究事業)
毛細血管拡張性小脳失調症の実態調査、早期診断法確立と、病態評価に関する研究班 編

内容